THE ASTROPHYSICAL JOURNAL, 209:214-232, 1976 October 1

STAR DISTRIBUTION AROUND A MASSIVE BLACK HOLE IN A GLOBULAR CLUSTER*

J. N. BAHCALL
Institute for Advanced Study

AND

R. A. WOLF
Institute for Advanced Study, and Rice University
Received 1975 December 29

ABSTRACT

In order to predict the likely distribution of stars around a massive black hole in the core of a cluster of stars, we derive an equation of the Fokker-Planck type that describes the diffusion of stars in the $1/r$ gravitational well of the black hole, by star-star gravitational collisions. The main assumptions are: (1) the distribution of stars is adequately described by a single-particle distribution function that is spherically symmetric in coordinate space and approximately isotropic in velocity space; (2) the stars have equal masses; (3) star mass $\ll$ black-hole mass $\ll$ cluster-core mass; (4) a star is destroyed by star-star collisions or by tidal forces when its binding energy in the well exceeds a specified large value; (5) binaries are unimportant. We calculate numerical solutions for the time-dependent equations. These solutions indicate that the equilibrium star density, closely approached within a collision time, approximates an $r^{-7/4}$ power law throughout most of the well. The same equilibrium power law obtains for nonisotropic distribution functions whose anisotropy is independent of r. Stars in bound orbits about a black hole diffuse down slowly into its gravitational well under equilibrium conditions. A black hole of $\leqslant 10^3\ M_\odot$ may accrete stars primarily by capture from unbound orbits.

We calculate the predicted shape of the star distribution near the cluster center that might be observed with small diaphragms. We also calculate, as a function of diaphragm size, the velocity dispersion and line profile that might be measured spectroscopically. Some calculations are also presented for an open slit configuration. We conclude that, for globular clusters in our Galaxy, one might be able to detect black holes with masses $\geqslant 5 \times 10^3\ M_\odot$ and, with a large space telescope, masses $\geqslant 10^3\ M_\odot$. We also present an approximate formula for the mean distance of a massive black hole from the center of mass of the unbound stars.

Subject headings: clusters: globular — stars: black holes — stars: stellar dynamics

I. INTRODUCTION

Theorists have felt for years that the cores of globular clusters were likely sites for massive black holes (see, e.g., Wyller 1970; Peebles 1972*a*), and this feeling has been strengthened recently by the discovery that several X-ray sources are associated with globular clusters (Giacconi *et al.* 1974; Clark, Markert, and Li 1975; Canizares and Neighbours 1975). Some models of these sources involve massive black holes (e.g., Bahcall and Ostriker 1975; Silk and Arons 1975). It therefore seems reasonable now to investigate in detail a question raised by Wyller (1970) and treated semiquantitatively by Peebles (1972*a*, *b*), namely, what would be the distribution of solar-mass stars around a massive black hole in the core of a star cluster?

The present work was motivated by, and in many ways follows, that of Peebles (1972*b*), who used dimensional reasoning to derive a power-law for the distribution function, f, describing stars in bound orbits about a black hole. We adopt his basic physical picture, wherein stars in bound orbits in the $-GM_{\rm BH}/r$ gravitational potential of the black hole diffuse from one bound orbit to another because of star-star gravitational scattering. We derive detailed expressions for the relevant diffusion coefficients and solve numerically the time-dependent Boltzmann equation. We find solutions that satisfy the boundary conditions at zero binding energy and large binding energy (the Peebles solution does not). Our results resemble somewhat those conjectured by Peebles in that when the system is near its equilibrium steady-state configuration (after roughly one relaxation time) the distribution function is then approximately a power law throughout most of the hole's gravitational well. However, we deduce a different energy power law than he did, $f(E) \propto E^{1/4}$ instead of $E^{3/4}$, and our solutions imply a lower equilibrium rate for accretion of stars onto the black hole from bound orbits. In constructing his scaling argument, Peebles assumed that the scattering rate into more bound orbits was independent of stellar energy and also independent of the energy, E_D, at which stellar coalescence (or tidal disruption) occurs. Our calculations show that the Peebles

* Research supported by National Science Foundation grant NSF-GP-40768X.

solution actually implies a very rapid rate of diffusion of stars *away* from the black hole (see discussion following eqs. [58] and [63]).

The reader who is primarily interested in observations may do best by turning directly to § V in which we discuss various methods of detecting massive black holes in the cores of globular clusters. We formulate the mathematical problem in § II, listing our principal assumptions and outlining our procedure. Most of our calculations are described in § III, in which we derive a time-dependent diffusion equation for an isotropic distribution function; obtain a simple zero-flow solution, $f \propto E^{1/4}$, that does not satisfy the "realistic" boundary conditions; present numerical solutions of the full time-dependent equation; and discuss the star accretion rate. In § IV we generalize our simple solutions to the case in which the distribution function is allowed to be a factorable function of energy and eccentricity. We calculate in § V the star distribution near the center of a star cluster and predict the star counts or photometric intensity that might be measured (cf. eq. [85]). We also derive expressions for the line profiles and velocity dispersions that may be observed spectroscopically with small diaphragms or slits (see especially Figs. 3 and 4). This section also contains estimates of what black-hole masses one might hope to detect in globular clusters with ground-based or space telescopes and an approximate formula for the mean distance of a massive black hole from the center of mass of the unbound stars. The expected large statistical fluctuations close to the black hole are discussed in § VI. The possible relevance of various stellar accretion processes for globular-cluster X-ray sources is discussed briefly in § VII.

II. FORMULATION

a) Assumptions

We list below our principal assumptions and approximations.

1. *The distribution of stars is adequately represented by a single-particle distribution function that is spherically symmetric in space and approximately isotropic in velocity space.* We follow Peebles (1972*a*) in using a single-particle distribution function (see § VI). In our detailed calculations we assume that the distribution function is approximately isotropic but show in § IV that our equilibrium power-law solution is also valid for a large class of nonisotropic distribution functions. The rate at which stars diffuse closer to the hole, a slow nonisotropic process, is calculated assuming the distribution function is isotropic, analogous to the calculation of radiative diffusion in stellar interiors using scalar quantities.
2. *The black-hole mass, $M_{\rm BH}$, is much less than M_c, the mass of the core of the globular cluster.*
3. *The stars around the hole all have the same mass M_*, which is small compared to $M_{\rm BH}$.*
4. *Only a small fraction of these stars are binaries.*
5. *The predominantly important collisions are those involving small changes in star velocity.* This assumption is standard in treating diffusion caused by an r^{-1} scattering potential (e.g., Rosenbluth, MacDonald, and Judd 1957).
6. *A star is destroyed if its binding energy per unit mass in the hole's gravitational wall exceeds $E_D \sim (GM_*/R_*)$,* because then direct contact collisions between stars become more important than distant gravitational encounters (see § III*e* and Frank 1976).

b) Some Implications

Our aim is to determine the stellar distribution function, $f(\boldsymbol{x}, \boldsymbol{v}, t)$, the number of stars per unit volume in coordinate space, per unit volume in velocity space. Given $f(\boldsymbol{x}, \boldsymbol{v}, t)$, the number density, mean-square velocity, etc., may be calculated straightforwardly.

Peebles (1972*b*) noted one great simplification that follows from assumptions 1 and 3, namely, that the isotropic part of the distribution function f can be written as a function of just E and t, where, following Peebles, we define E to be minus the stellar energy per unit mass:

$$E = GM_{\rm BH}/r - \tfrac{1}{2}v^2 \tag{1}$$

with v = stellar velocity and r = distance from black hole. We indicate below the explicit ideas and approximations that lead to the result $f \approx f(E, t)$.

We first note that assumption 2 implies that τ_c, the stellar collision time, is long compared with T, the orbital period. We write

$$\frac{\tau_c}{T} \sim \frac{v^3 n^{-1}(GM_*)^{-2}}{rv^{-1}}, \tag{2}$$

where n = number density of stars. As a typical velocity, we adopt $\langle \Delta v^2 \rangle^{1/2}$, the measured velocity dispersion *along the line of sight* in the core of the cluster. For a typical radius, we take $r = r_h$ (the characteristic gravitational capture radius), where (Peebles 1972*b*)

$$r_h = GM_{\rm BH}\langle \Delta v^2 \rangle^{-1}. \tag{3}$$

For a typical density, we take n equal to n_0, the number density of stars in the cluster's core, thus obtaining

$$\frac{\tau_c}{T} \sim \frac{\langle \Delta v^2 \rangle^2}{r_h n_0 (GM_*)^2}\,. \tag{4}$$

Eliminating r_h from equation (4) using (3) and using the definition of a core mass,

$$M_c = \tfrac{4}{3}\pi n_0 r_c^3 M_*\,, \tag{5}$$

yields

$$\frac{\tau_c}{T} \sim \frac{\langle \Delta v^2 \rangle^3 r_c^3}{G^3 M_{\rm BH} M_* M_c}\,. \tag{6}$$

Using the inferred relation (Peterson and King 1975) that

$$GM_c/r_c \sim \langle \Delta v^2 \rangle \tag{7}$$

in globular clusters, and then assumption 2, leads to the desired result

$$\frac{\tau_c}{T} \sim \frac{M_c^2}{M_* M_{\rm BH}} \gg 1\,. \tag{8}$$

It might be argued that the above "typical" choices for r, n, and v are actually not typical deep down in the well. However, our procedure is self-consistent: *solutions obtained assuming $\tau_c \gg T$ imply that τ_c/T increases with decreasing r.*

The ratio τ_c/T is typically $\gtrsim 10^6$ in the situations we consider. Thus we can assume consistently that the flow-associated anisotropic part of the distribution function is of the order of 10^{-6} of the isotropic part, and we neglect anisotropy in computing collision rates and related quantities.

The Boltzmann equation implies that, in the absence of collisions, the distribution function f is constant along the trajectory of a particle in phase space, and this constancy holds approximately in our problem because of equation (8). Thus, $f(\boldsymbol{r}_a, \boldsymbol{v}_a, t) = f(\boldsymbol{r}_b, \boldsymbol{v}_b, t)$ if $(\boldsymbol{r}_a, \boldsymbol{v}_a)$ and $(\boldsymbol{r}_b, \boldsymbol{v}_b)$ both lie on the same orbital path, and, neglecting anisotropy of f, directions are irrelevant, so that

$$f(r_a, v_a, t) = f(r_b, v_b, t)\,. \tag{9}$$

The only restriction, given our assumptions of isotropy and no collisions, on the validity of equation (9) is that (r_a, v_a) and (r_b, v_b) correspond to the same energy. Thus f is a function of just E and t.

Assumption 2 implies another simplification, namely, that the gravitational potential for $r \lesssim r_h$ is, within an additive constant, approximately equal to $-GM_{\rm BH}/r$, because the total mass of stars at $r \lesssim r_h$ is much less than $M_{\rm BH}$, i.e.,

$$\frac{M_*}{M_{\rm BH}} \int_0^{r_h} 4\pi r^2 n(r) dr \ll 1\,. \tag{10}$$

The correctness of equation (10) can easily be verified by taking a "typical value" $n = n_0$, then using equations (5) and (7) with assumption 2. The use of $n = n_0$ can be checked *a posteriori* for self-consistency: in all of our solutions n is a sufficiently weak function of r that

$$\int_0^{r_h} r^2 n(r) dr \sim n_0 \int_0^{r_h} r^2 dr\,. \tag{11}$$

A further implication of the assumptions is that the radius, $r_D \sim GM_{\rm BH}/E_D$, at which stellar disruption occurs is much smaller than r_h, i.e.,

$$r_D/r_h \sim R_* \langle \Delta v^2 \rangle / GM_*\,. \tag{12}$$

In typical rich clusters, $\langle \Delta v^2 \rangle \sim 50\ \rm km^2\ s^{-2}$ and $GM_*/R_* \sim 2 \times 10^5\ \rm km^2\ s^{-2}$. Thus

$$r_D/r_h \sim 2 \times 10^{-4}\,. \tag{13}$$

The region where stars remain intact but have their motion dominated by the gravitational field of the well thus spans several orders of magnitude in both r and E.

c) *Outline of Procedure, Boundary Conditions*

We first calculate, in terms of the distribution function $f(E, t)$, the net rate $R(E, t)$ at which stars flow diffusively through energy level E toward higher E-values (more tightly bound orbits). Then we use conservation of particles to derive a diffusion equation for the system, an equation expressing $\partial f(E, t)/\partial t$ in terms of $\partial R(E, t)/\partial E$. Starting from an arbitrarily chosen initial condition, $f(E, 0)$, we step the diffusion equation along in time until the system comes to equilibrium. As a boundary condition, we require

$$f(E, t) = n_0[2\pi\langle\Delta v^2\rangle]^{-3/2} \exp\left[\frac{E}{\langle\Delta v^2\rangle}\right] \tag{14}$$

for $E < 0$, because the distribution functions in the cores of globular clusters are presumed to be nearly Maxwellian. Since the stars are disrupted for $E > E_D$, we get

$$f(E_D, t) = 0\,, \tag{15}$$

and do not calculate f for higher E-values. The imposition of the boundary condition (15) forces the solution to be far from a Maxwell-Boltzmann distribution, since the solution for thermal equilibrium requires many stars near the black hole.

III. EQUATIONS FOR AN ISOTROPIC DISTRIBUTION FUNCTION

a) Calculation of the Scattering Rate

Consider first an elementary collision in which the velocity of star a changes from $\boldsymbol{v}_a$ to $\boldsymbol{v}_a'$ and the velocity of star b changes from $\boldsymbol{v}_b$ to $\boldsymbol{v}_b'$. It is convenient to discuss the collision in terms of relative and center-of-mass velocities:

$$\boldsymbol{V}_R = \boldsymbol{v}_a - \boldsymbol{v}_b \tag{16a}$$

and

$$\boldsymbol{V}_M = \tfrac{1}{2}(\boldsymbol{v}_a + \boldsymbol{v}_b)\,, \tag{16b}$$

with analogous definitions for V_R' and V_M'. Also define

$$E_a = GM_{\rm BH}/r - \tfrac{1}{2}v_a^2\,, \tag{17a}$$

$$E_a' = GM_{\rm BH}/r - \tfrac{1}{2}(v_a')^2\,, \tag{17b}$$

with analogous definitions for E_b, E_b'.

The function $R(E, t)$ is the number of stars per unit time that are scattered into a region of energy greater than E by two-particle collisions. The number of collisions in volume d^3r per unit time causing transitions from volume $d^3v_a d^3v_b = d^3V_R d^3V_M$ in two-particle velocity space to volume $d^3v_a' d^3v_b' = d^3V_R' d^3V_M'$ is

$$d^3r d^3V_R d^3V_M d^3V_R' d^3V_M' \cdot V_R(d\sigma/d\Omega) f(E_a, t) f(E_b, t) \delta^{(3)}(V_M' - V_M)\delta(V_R' - V_R)(V_R')^{-2}\,,$$

where $d\sigma/d\Omega$ is the differential scattering cross section. For convenience in performing the integrals, we have written $d\sigma/d\Omega\; d\Omega$ as

$$\int d^3V_R' \frac{\delta(V_R - V_R')}{V_R'^2}\left(\frac{d\sigma}{d\Omega}\right).$$

With d^3V_R and d^3V_R' written out in terms of magnitudes and directions, we integrate over all collisions to obtain

$$\begin{aligned} R(E, t) = \int d^3r \int V_R^2 dV_R \int d^2\Omega_R \int dV_R' \int d^2\Omega_R' \int d^3V_M \int d^3V_M' \\ \times V_R(d\sigma/d\Omega) f(E_a, t) f(E_b, t) \delta^{(3)}(V_M' - V_M)\delta(V_R' - V_R) S\,, \end{aligned} \tag{18}$$

where

$$S = \tfrac{1}{4}[\mathrm{sign}\,(E_a' - E) + \mathrm{sign}\,(E_b' - E) - \mathrm{sign}\,(E_a - E) - \mathrm{sign}\,(E_b - E)] \tag{19}$$

is $+1$ for transitions crossing E to higher energies, -1 for transitions crossing E to lower energies, and zero for all other collisions. A factor of $\frac{1}{2}$ has been included to avoid counting each reaction twice.

A change of variables is convenient:

$$d^3V_M d^3V_M' \to (V_R V_R')^{-1} dE_a dE_a' dE_b dE_b' d\Phi d\Phi'\,, \tag{20}$$

where Φ is the azimuthal angle between V_M and the $V_R V_R'$ plane; Φ' is the azimuthal angle between V_M' and the $V_R V_R'$ plane. Substituting (20) in (18), writing $\delta^{(3)}(V_M' - V_M)$ in terms of spherical polar coordinates, and integrating V_R' yields

$$\begin{aligned} R(E, t) = 2\int dE_a \int dE_b \int dE_a' \int dE_b' \delta(E_a' + E_b' - E_a - E_b) \int d^3r \int V_R dV_R \int d^2\Omega_R \int d^2\Omega_R' \\ \times \frac{d\sigma}{d\Omega}(V_R, \hat{\Omega}_R' - \hat{\Omega}_R) f(E_a, t) f(E_b, t) S P[2GM_{\rm BH} r^{-1} - E_a - E_b - V_R^2/4]^{-1/2}\,, \end{aligned} \tag{21}$$

where

$$P = \int d\Phi \int d\Phi' \delta^{(2)}(\hat{\Omega}_M' - \hat{\Omega}_M) \tag{22}$$

is an integral that is easily worked out:

$$P = 2[\sin^2 \theta \sin^2 \alpha - (\cos \theta' - \cos \theta \cos \alpha)^2]^{-1/2} . \tag{23}$$

Here θ is the scattering angle (between V_R and V_R'); α is the angle between V_R and V_M; and θ' is the angle between V_R' and V_M'. One must perform some algebraic and trigonometric steps to obtain equation (23) since α and θ' are measured with respect to different axes. The bracketed term in equation (23) must be positive for a scattering process that satisfies the conservation laws, a requirement that determines the limits of integration in some of the following equations.

If we make the small-scattering-angle approximation (assumption 5) and write α and θ' in terms of V_R and the energies, we obtain

$$P \approx 2V_R E_M^{1/2}\{\theta^2[V_R^2 E_M - (E_b' - E_a')(E_b - E_a)] - (E_b - E_a - E_b' + E_a')^2\}^{-1/2} , \tag{24}$$

where

$$E_M = 2GM_{\rm BH}r^{-1} - E_a - E_b - \tfrac{1}{4}V_R^2 . \tag{25}$$

In the approximation of small scattering angles, the scattering formula is

$$\frac{d\sigma}{d\Omega} \approx \frac{16G^2M_*^2}{V_R^4\theta^4} , \tag{26}$$

and we have

$$R(E, t) = 128\pi G^2 M_*^2 \int dE_a \int dE_b \int dE_a' \int dE_b' \delta(E_a + E_b - E_a' - E_b') S f(E_a, t) f(E_b, t)$$
$$\times \int d^3r \int d^2\Omega_R \int V_R^{-2} dV_R I[V_R^2 E_M - (E_b' - E_a')(E_b - E_a)]^{-1/2} , \tag{27}$$

where

$$I = (2\pi)^{-1} \int d^2\Omega_R' \theta^{-4}[\theta^2 - \theta_m^2]^{-1/2} , \tag{28}$$

$$\theta_m^2 = (E_b - E_a - E_b' + E_a')^2[V_R^2 E_M - (E_b' - E_a')(E_b - E_a)]^{-1} . \tag{29}$$

Note that θ_m^2 must be positive if there is a solution to the scattering problem for the variables indicated. The integral I is easy to evaluate within assumption 5, which implies $\theta_m \ll 1$. The integral over V_R is also simple, and the integrations over $d^2\Omega_R$ and the direction of $\boldsymbol{r}$ contribute just a factor $(4\pi)^2$. We obtain

$$R(E, t) \approx \frac{32\pi^4}{3} G^2 M_*^2 \int dE_a \int dE_b \int dE_a' \int dE_b' \delta(E_a + E_b - E_a' - E_b') S f(E_a, t) f(E_b, t) |\Delta|^{-3} K , \tag{30}$$

where

$$\Delta = E_a' - E_a = E_b - E_b' , \tag{31}$$

$$K = \int_0^{r_{\max}} r^2 dr (V_{R\max} - V_{R\min})^3 , \tag{32}$$

$$\begin{Bmatrix} V_{R\max} \\ V_{R\min} \end{Bmatrix} = 2^{1/2}[2GM_{\rm BH}r^{-1} - E_a - E_b \pm \{(2GM_{\rm BH}r^{-1} - E_a - E_b)^2 - (E_b - E_a)(E_b' - E_a')\}^{1/2}]^{1/2} \tag{33}$$

and

$$r_{\max} = 2GM_{\rm BH}\{E_a + E_b + [(E_b - E_a)(E_b' - E_a')]^{1/2}\}^{-1} . \tag{34}$$

The indicated limits on V_R result from the requirement that θ_m^2 be positive.

The integral K is easily calculated once one realizes that $(V_{R\max} - V_{R\min})^2$ has a simple form. One finds

$$K = 4\pi G^3 M_{\rm BH}^3\{E_a + E_b + [(E_b - E_a)(E_b' - E_a')]^{1/2}\}^{-3/2} , \tag{35}$$

an expression that we can simplify by noting that assumption 5 implies

$$E_b' - E_a' \approx E_b - E_a . \tag{36}$$

Since S is antisymmetric under interchange of initial and final states while everything else is symmetric, we can replace $f(E_a, t)f(E_b, t)$ by $\frac{1}{2}[f(E_a, t)f(E_b, t) - f(E_a', t)f(E_b', t)]$; we can expand this expression in powers of the small energy change Δ. This manipulation is convenient because of the apparent singularity at small energy exchanges, Δ. Utilizing also the symmetry between a and b, we write

$$R(E, t) \approx (8\sqrt{2\pi^5}/3)G^5 M_*^2 M_{\rm BH}^3 \int dE_b \int dE_a [\max(E_a, E_b)]^{-3/2} \times [f(E_a, t)\partial f(E_b, t)/\partial E_b - f(E_b, t)\partial f(E_a, t)/\partial E_a]L\,, \tag{37}$$

where max (x, y) is the larger of x and y, and

$$L = \int_{-\infty}^{E_D} d\Delta\Delta|\Delta|^{-3}[\operatorname{sign}(E_a + \Delta - E) - \operatorname{sign}(E_a - E)] = 2|E_a - E|^{-1}\,. \tag{38}$$

The integral over E_a formally diverges because of the singularity at $E_a = E$, so we introduce a small cutoff energy, $\Delta_{\min}$, and a maximum energy, $E_{\max}$, at which collisions are important. For a well-behaved function $H(E_a)$,

$$\int \frac{dE_a}{|E_a - E|} H(E_a) = 2H(E) \ln \Lambda\,, \tag{39}$$

where $\Lambda = E_{\max}/\Delta_{\min}$. We obtain, finally, for the net rate at which stars diffuse through "energy" E,

$$R(E, t) \approx (32 \times 2^{1/2}\pi^5/3)G^5 M_{\rm BH}^3 M_*^2 \ln \Lambda \int dE_b [\max(E, E_b)]^{-3/2} \times [f(E, t)\partial f(E_b, t)/\partial E_b - f(E_b, t)\partial f(E, t)/\partial E]\,. \tag{40}$$

The lower limit cutoff in equation (39) results from the requirement that the collision time at the maximum effective impact parameter, $b_{\max}$, be smaller than the orbital period of the bound star. The momentum transfer at $b_{\max}$ is of order $(GM_*^2/b_{\max}v)$, leading to a minimum energy transfer from orbits of energy E of order $(M_*/M_{\rm BH})E$. The maximum energy transfer, because of our small angle approximation, is of order E. Thus

$$\Lambda \sim M_{\rm BH}/M_*\,. \tag{41}$$

In analogous problems in plasma physics, the maximum impact parameter is the Debye–Hückel shielding radius. For gravitational collisions that determine stellar relaxation times, the maximum impact parameter is the characteristic size of the system (see, e.g., Cohen, Spitzer, and Routly 1950). In the presence of a dominant central potential, our cutoff is more severe than either of the above.

b) *Time-Dependent Diffusion Equation*

The number of stars with "energies" between E and $E + dE$ is defined to be $N(E, t)dE$, and is related to $f(E, t)dE$ as follows:

$$N(E, t)dE = \int d^3r \int d^3v f(E, t)\delta(GM_{\rm BH}/r - \tfrac{1}{2}v^2 - E)dE = \pi^3 2^{1/2} G^3 M_{\rm BH}^3 E^{-5/2} f(E, t)dE\,. \tag{42}$$

Conservation of stars requires $dN(E, t)dE = dt[R(E, t) - R(E + dE, t)]$ or

$$\partial N(E, t)/\partial t = -\partial R(E, t)/\partial E\,, \tag{43}$$

which, with equations (40) and (42), becomes

$$\frac{\partial f(E, t)}{\partial t} = -AE^{5/2}\frac{\partial}{\partial E}\left\{\int dE_b \frac{f(E, t)\partial f(E_b, t)/\partial E_b - f(E_b, t)\partial f(E, t)/\partial E}{[\max(E, E_b)]^{3/2}}\right\}, \tag{44}$$

where

$$A = (32\pi^2/3)G^2 M_*^2 \ln \Lambda\,. \tag{45}$$

Equation (44) is the basic diffusion equation governing stars in bound orbits around the black hole. We now rewrite it in a dimensionless form, and a Fokker-Planck form.

Since f is Maxwellian for "energy" $E < 0$, it is useful to adopt dimensionless variables based on this boundary condition:

$$g = (2\pi\langle\Delta v^2\rangle)^{3/2} n_0^{-1} f; \tag{46}$$

$$x = E\langle\Delta v^2\rangle^{-1}; \qquad y = E_b\langle\Delta v^2\rangle^{-1}; \tag{47}$$

$$\tau = A n_0 (2\pi\langle\Delta v^2\rangle)^{-3/2} t. \tag{48}$$

The unit of time, $(2\pi\langle\Delta v^2\rangle)^{3/2} A^{-1} n_0^{-1}$, introduced in equation (48) is of order one-half the relaxation times defined by Spitzer and Hart (1971) and Chandrasekhar (1942) for the region $r > r_h$ (although the meaning of some of our symbols is necessarily different from the usage of previous authors). Equation (44) becomes

$$\frac{\partial g(x, \tau)}{\partial \tau} = -x^{5/2} \frac{\partial Q(x, \tau)}{\partial x}, \tag{49a}$$

where the dimensionless rate-integral, Q, is defined as

$$Q(x, \tau) = \int_{-\infty}^{x_{\max}} dy[g(x, \tau)\partial g(y, \tau)/\partial y - g(y, \tau)\partial g(x, \tau)/\partial x] \max(x, y)^{-3/2}. \tag{49b}$$

Equation (49) holds for $0 < x < x_m$. We specify

$$g(x, \tau) = e^x, \qquad x < 0; \tag{50}$$

$$g(x, \tau) = 0, \qquad x \geq x_{\max}, \tag{51}$$

where

$$x_{\max} = E_D\langle\Delta v^2\rangle^{-1}. \tag{52}$$

Numerical solutions to (49) are presented in § III*e*.

It is clear, *a priori*, that $N(E, t)$ must satisfy a one-dimensional Fokker-Planck equation

$$\frac{\partial N(E, t)}{\partial t} = -\frac{\partial}{\partial E}\{N(E, t)c_1(E, t)\} + \frac{1}{2}\frac{\partial^2}{\partial E^2}\{N(E, t)c_2(E, t)\}, \tag{53}$$

because this form follows from assumption 5 and conservation of particles (stars). (See, for example, Chandrasekhar 1943.) Using (42) and a moderate amount of straightforward algebra, one can show that (44) and (53) are equivalent if

$$c_1(E, t) = \langle\Delta E/\Delta t\rangle = (3/2)A\left\{\int_E^{\infty} (E/E_b)^{5/2} f(E_b, t)dE_b - \int_{-\infty}^{E} f(E_b, t)dE_b\right\}, \tag{54}$$

$$c_2(E, t) = \langle\Delta E^2/\Delta t\rangle = 2AE^{5/2}\int_{-\infty}^{\infty} f(E_b, t)[\max(E, E_b)]^{-3/2} dE_b. \tag{55}$$

c) Power-law Equilibrium Solutions

We are interested in equilibrium solutions with $\partial f/\partial t = 0$. It is, of course, immediately evident from (40) that a Boltzmann distribution, $f(E) = C\exp(M_* E/kT)$, implies $R(E, t) = 0$ and thus $\partial f/\partial t = 0$. However, as Peebles (1972*b*) has argued, this distribution implies enormous densities deep in the well, which would be destroyed by tidal breakup or coalescence (cf. the boundary condition of eq. [15]).

Following Peebles (1972*b*), we first consider equilibrium solutions ($\partial f/\partial t = 0$) in which the distribution function has a power-law form,

$$f(E) = CE^p, \tag{56}$$

and $R(E)$ has a nonzero value that is independent of E. Such solutions do not satisfy our boundary conditions (14) or (15); however, the solution that satisfies the boundary conditions might be expected to lie close to the power-law solution for $r_D \ll r \ll r_h$ and, because r_D is very much smaller than r_h, this is a physically interesting domain. Substituting (56) in (40) gives

$$R(E) = \text{constant} = D\int_0^{\infty} dE_b[\max(E, E_b)]^{-3/2}\{E^p E_b^{p-1} - E_b^p E^{p-1}\}, \tag{57}$$

$$= DE^{2p-3/2}\int_0^{\infty} dz[\max(1, z)]^{-3/2}\{z^{p-1} - z^p\}. \tag{58}$$

Thus, if $R(E)$ = nonzero constant, then $p = \frac{3}{4}$; this was the conclusion reached by Peebles (1972*b*) and was the basis for his $f(E) = CE^{3/4}$ power law. However, equation (58) reveals a problem with the Peebles law, namely, the z^p term in the integrand is proportional to $z^{-3/4}$ as z goes to infinity; the integral thus diverges at its upper limit. The constant value of $R(E)$ is therefore minus infinity. A solution that is close to $CE^{3/4}$ (except near the boundaries) implies very rapid diffusion *away* from the black hole.

We have found another power-law solution that corresponds to *zero flow*, $R(E) = 0$ for all E. Adopting form (56) again, we require

$$0 = \int_0^\infty dE_b[\max(E, E_b)]^{-3/2}[E^p E_b^{p-1} - E_b^p E^{p-1}]$$

or

$$0 = p^{-1} - (p+1)^{-1} + (\tfrac{3}{2} - p)^{-1} - (\tfrac{1}{2} - p)^{-1} . \qquad (59)$$

Within the range where the integral converges, $0 < p < \frac{1}{2}$, there is one solution:

$$p = 1/4 , \qquad \text{i.e.,} \qquad f = CE^{1/4} . \qquad (60)$$

Thus $f(E) = CE^{1/4}$ is an equilibrium solution to the diffusion equation.

We note that this solution also gives zero when substituted into the right-hand side of equation (37), an expression for R that (unlike [40]) is not subject to small errors caused by our sloppy treatment of the cutoff parameter Λ. This result is readily verified by substituting equation (60) into (37) and reversing the order of integration.

d) Numerical, Time-dependent Solutions

We have solved equation (49) numerically for the dimensionless distribution function $g(x, \tau)$, for several values of $x_{\max}$, starting in each case from an arbitrary initial condition. Results from two such calculations are shown in Figures 1 and 2.

Note the following features:

i) In the two cases shown, the initial distribution function was much smaller than the equilibrium value through most of the well; and the potential well started to fill up, first near the top ($0 < x \ll x_{\max}$), then the bottom ($x \sim x_{\max}$).

ii) The distribution function changes rapidly for the first one unit of dimensionless time, but very slowly after $\tau = 1$; the function seems to approach quickly an equilibrium curve.

iii) For $1 \ll x \ll x_{\max}$, the equilibrium distribution function is within a factor of 2 of the simple power-law solution:

$$g = 2x^{1/4} . \qquad (61)$$

As g approached its equilibrium form, the dimensionless rate integral Q appeared to approach a constant value of approximately 7×10^{-2} for $x_{\max} = 10^2$ and 8×10^{-4} for $x_{\max} = 10^4$.

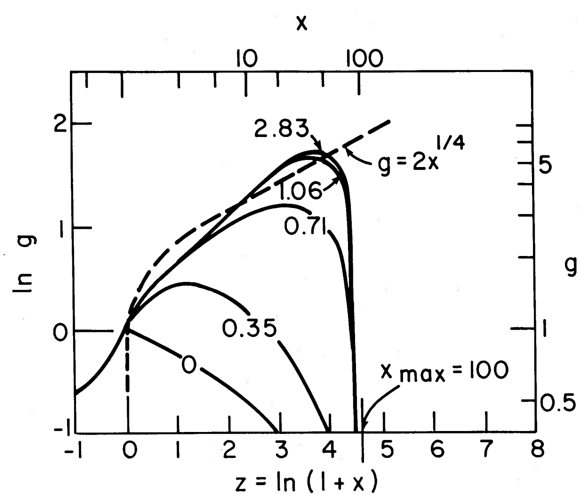

FIG. 1.—Dimensionless distribution function g plotted as a function of dimensionless binding energy x, for the case where the star breakup point is $x_{\max} = 100$. The numbers on the curves are dimensionless times τ. Also plotted for comparison is an $x^{1/4}$ power law.

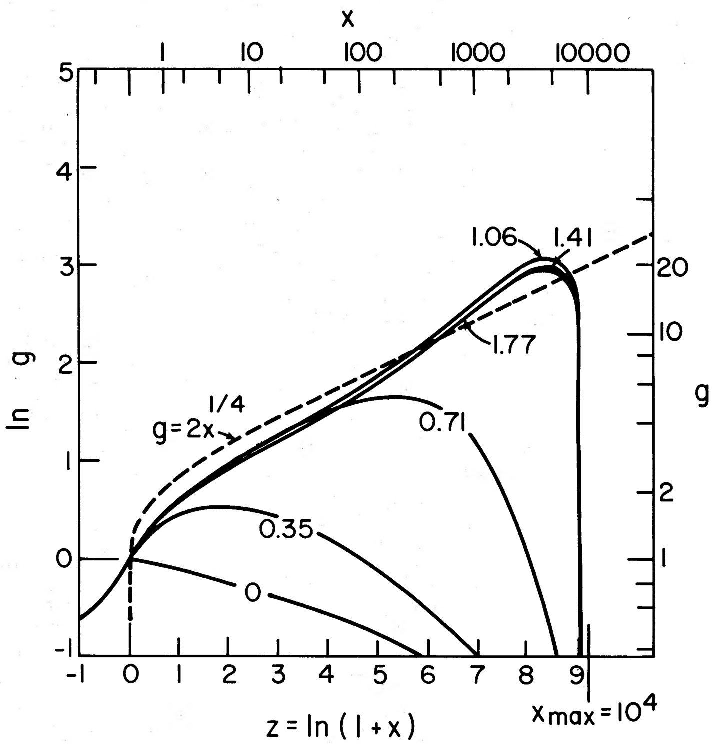

FIG. 2.—Dimensionless distribution function g plotted as a function of dimensionless binding energy x, for the case $x_{\max} = 10^4$. The numbers on the curves are dimensionless times τ (see eq. [48] of the text).

Our calculations, based on the assumption that f is isotropic, indicate that the relaxation proceeds on a time scale less than half of Chandrasekhar's relaxation time t_E, applied to the core of the cluster, neglecting the black hole. To see why, consider the energy diffusion coefficient $\langle \Delta E^2/\Delta t\rangle$ as a function of position for $r \lesssim r_h$. The coefficient is of the order of $\nu\langle K^2\rangle$, where ν = local collision frequency and $\langle K^2\rangle$ = local average of the square of the stellar kinetic energy. The collision frequency increases slightly with decreasing r and $\langle K^2\rangle$ increases rapidly, like r^{-2}. Consider the effect of this on a typical $x = 1$ ($E = \langle \Delta v^2\rangle$) star. Most such stars penetrate to radial distances several times smaller than r_h, and consequently feel, on parts of their orbits, diffusion coefficients $\langle \Delta E^2/\Delta t\rangle$ much larger than the ones felt by a typical cluster star that is not influenced by the gravitational field of the black hole.

e) The Equilibrium Flow Rate and Other Accretion Rates

The relationship between $R(E, t)$, the flow rate, and the dimensionless integral $Q(x, t)$ can be written

$$R(E, t) = \pi 2^{-3/2} R_0 Q(x, t)\,, \tag{62a}$$

where

$$R_0 = \frac{4\pi}{3} r_h^3 n_0 \frac{4G^2 M_*^2 \ln \Lambda n_0}{\langle \Delta v^2\rangle^{3/2}}\,, \tag{62b}$$

which is of the order of the number of stars in the hole (with $r < r_h$) divided by a mean collision time for the cluster. Numerically

$$R_0 \sim 6 \times 10^{-7}\,\mathrm{yr}^{-1}\,(M_{\mathrm{BH}}/10^3\,M_\odot)^3 (n_0/5 \times 10^4\,\mathrm{pc}^{-3})^2 (10\,\mathrm{km\,s}^{-1}/\langle \Delta v^2\rangle^{1/2})^9\,. \tag{62c}$$

Although Q was generally ~ 1 for $x \sim 1$ early in our numerical experiments, the asymptotic values we obtained approximately satisfied the relation

$$Q(x, \infty) \approx 8 x_{\max}^{-1} \approx 8\langle \Delta v^2\rangle/(E_D)\,, \tag{63}$$

independent of x. But in (49b), each of the two terms in the integral expression for Q has a magnitude $\sim 3x^{-1}$, for $1 \ll x \ll x_{\max}$ and $g \approx 2x^{1/4}$. Far from $x_{\max}$, the two terms almost exactly cancel each other. However, near $x_{\max}$ the two terms diverge from each other, the approximate cancellation no longer occurs, and the net flow rate is of the same order of magnitude as the larger of the two terms. The bottleneck for the diffusive flow occurs near $E \approx E_D$. For $\langle \Delta v^2 \rangle \ll E \ll E_D$, the flow rate could conceivably have been much higher, considering the number densities, mean energy, and available volume; however, to maintain a steady state, the distribution function in this energy range tends toward the $E^{1/4}$ form in which the flow rate is zero.

The energy flow rate (away from the black hole) is $R(E, \infty)E_D$, which is practically independent of energy with our approximations (see eqs. [62a] and [63]). The distribution function far from the black hole does not depend much on E_D, so it is natural that the heat flux must also be practically independent of E for $E \ll E_D$.

For the dimensional flow rate $R(E, \infty)$, we obtain, from (62) and (63) ($x_{\max} \sim 1.9 \times 10^3$)

$$R(E, \infty) \approx (30 \text{ stars per } 10^{10} \text{ yr}) \times \left(\frac{M_{\rm BH}}{10^3 M_\odot}\right)^3 \left(\frac{M_*}{1 M_\odot}\right)^2 \left(\frac{\ln \Lambda}{10}\right) \left\langle \left(\frac{\Delta v}{10 \text{ km s}^{-1}}\right)^2 \right\rangle^{-7/2} \times \left(\frac{n_0}{5 \times 10^4 \text{ pc}^{-3}}\right)^2 (GM_\odot/R_\odot E_D)\,, \tag{64}$$

a slow rate under expected globular-cluster conditions.

The equilibrium flow rate calculated above probably does not represent the dominant contribution to mass accretion by the black hole; tidal breakup from unbound orbits (and perhaps capture from "loss-cone" bound orbits) are apparently more rapid processes. The capture, and tidal breakup, of stars from *unbound* orbits that happen to take them within a tidal radius of the black hole can be estimated using the static approximation. One finds an accretion rate

$$R_{\rm tidal} = 2\pi r_T (GM_{\rm BH} n_0) v^{-1} \sim 10^{-7.5} \text{ yr}^{-1} \left\{ \left(\frac{M_{\rm BH}}{10^3 M_\odot}\right)^{4/3} \left(\frac{n_0}{5 \times 10^4 \text{ pc}^{-3}}\right) \left(\frac{10 \text{ km s}^{-1}}{\langle \Delta v^2 \rangle^{1/2}}\right) \left[\frac{r_T}{R_\odot} \left(\frac{M_\odot}{M_{\rm BH}}\right)^{1/3}\right] \right\}, \tag{65}$$

where r_T is the distance from the black hole at which tidal disruption occurs. Assuming that, at the beginning of the disruption process, the star traverses its orbit sufficiently slowly for hydrostatic equilibrium to obtain, one has $r_T \sim R_*(M_{\rm BH}/M_*)^{1/3}$, where R_*, M_* are the radius and mass of the star. Crude estimates suggest that this requirement is satisfied for most, or all, impact parameters of interest, but detailed dynamical calculations are obviously desirable (for other estimates of this rate, cf. Hills 1975 and Bahcall and Ostriker 1975). Frank (1976) has pointed out that the tidal radius r_T is much smaller than the stellar coalescence radius, r_D [$r_T/r_D \sim (M_*/M_{\rm BH})^{2/3}$], and hence E_D is the relevant energy at which to set our inner boundary condition.

Another important process is the capture of stars that have been scattered from simple bound orbits into "loss-cone" bound orbits, i.e., bound orbits with $E \ll GM_{\rm BH}/r_T$ that are so highly eccentric that they come within r_T of the black hole. Although we have no dependable quantitative formula for this capture rate R_B, it is probably small compared to R_0, the number of stars with $r < r_h$ divided by the mean collision time, because it involves scattering into a small solid angle. The rate R_B should be smaller than our numerically computed rates R until the system comes near equilibrium, when R_B probably becomes greater than R. This uncertainty about R_B does not affect our conclusions that f approximates an $E^{1/4}$ power law, but it means that the difference between one of our computed long-time distribution functions and the $E^{1/4}$ power law may not be a quantitatively accurate approximation to the difference between the actual system's asymptotic distribution function and the $E^{1/4}$ power law.

IV. ANISOTROPIC DISTRIBUTION FUNCTIONS

a) Motivation

We have considered so far collisional transitions between nearby energy levels on the assumption that the velocity-space distribution function within an energy level is isotropic except for the tiny correction due to the flow toward the black hole. We know this assumption must break down at some level of approximation (see the discussion of loss-cone effects above). A rigorous and straightforward approach to the anisotropic-velocity problem would be to let f be a function of orbital eccentricity ϵ, as well as E and t, and to balance particles going in and out of each state of given E and ϵ. But, with our present formalism, this approach entails an impracticably long calculation, and we have instead carried out a more restricted calculation with simplifying assumptions.

We found that in the isotropic case the system converged to an asymptotic solution in the order of a relaxation time, and we therefore consider now only asymptotic solutions. We also found that the asymptotic isotropic solution for "realistic" boundary conditions ([14] and [15]) was approximated closely by a simple solution ($f \propto E^{1/4}$) for the "easy" boundary conditions ($f \to 0$ as $E \to 0$, $f \to \infty$ as $E \to \infty$, $R = 0$) for most of the region of interest. Therefore, we adopt the "easy" boundary conditions for our discussion of the more complicated anisotropic case. For these "easy" boundary conditions, the problem has no intrinsic energy or length scale, and we expect that the fundamental solution, $f(t \to \infty)$, should have the same symmetry; specifically, it should be a separable function of E and ϵ. We define an eccentricity parameter

$$\lambda = (1 - \epsilon^2)/2 \tag{66}$$

and write

$$f(E, \epsilon, r) = h(E)u(\lambda)\,, \tag{67}$$

where $u(\lambda)$ = arbitrary function of λ. Equation (67), of course, does not apply to radii r that are inaccessible to a star of "energy" E, eccentricity ϵ; $f = 0$ in such forbidden regions.

We can show that setting $h(E) = CE^{1/4}$ for $E > 0$, $h(E) = 0$ for $E \le 0$, yields a flow rate $R(E)$ that is zero for all E; it thus represents a stationary state. The proof, which we outline briefly below, requires assumptions 2 through 5 and equation (67).

b) *Outline of Proof*

We list below a series of steps by which one can show that the factorable f of equation (67) is a solution of the anisotropic problem outlined above.

First, we rewrite equation (18) using the form (67) for the distribution function. Next we make two changes of variables, computing two Jacobians:

$$d^3V_R d^3V_M \to J_1 dE_a dE_b d\lambda_a d\lambda_b d\psi_a d\psi_b\,, \tag{68}$$

where ψ_a and ψ_b are the azimuthal angles, about the radial direction, of $\boldsymbol{v}_a$ and $\boldsymbol{v}_b$; also,

$$d\Phi_R' dV_R' \to J_2 dE_a' dE_b'\,, \tag{69}$$

where Φ_R' = azimuthal angle, about the radial direction, of V_R'. Next, we do the integral over V_M' using the momentum-conservation delta function, and convert $\delta(V_R' - V_R)$ to an energy delta function. Then, we use equation (26), and the assumption of small scattering angle (assumption 5), to perform the integration over θ. We make repeated use of assumption 5 to express R in the form

$$R(E) = 16\pi^4 G^5 M_{\rm BH}{}^3 M_*{}^2 C^2 \int dE_a \int dE_b \int dE_a' \int dE_b' (E_a E_b)^{-1/2} S\delta(E_a' + E_b' - E_a - E_b)|\Delta|^{-3} P(E_a, E_b, \lambda_m)\,, \tag{70}$$

where

$$P(E_a, E_b, \lambda_m) = \frac{GM_{\rm BH}}{8\pi^2(E_a E_b)^{1/4}} \sum_{\pm} \int \frac{dr}{r^2} \int d\lambda_a u(\lambda_a) \int d\lambda_b u(\lambda_b) \int d\psi_a \int d\psi_b \times (V_M \times V_R)^2 V_R^{-3} |(\boldsymbol{v}_a \cdot \hat{r})(\boldsymbol{v}_b \cdot \hat{r})|^{-1}\,, \tag{71}$$

and $\hat{r}$ is a unit vector in the radial direction. The sum is over two cases, $(\boldsymbol{v}_a \cdot \hat{r})(\boldsymbol{v}_b \cdot \hat{r}) > 0$ and $(\boldsymbol{v}_a \cdot \hat{r})(\boldsymbol{v}_b \cdot \hat{r}) < 0$. Any parameters involved in the definition of the arbitrary functions $u(\lambda)$ are symbolized by λ_m. The function P obviously has no dependence on final-state parameters, and all of the initial-state parameters are integrated over, except E_a and E_b. The factor $GM_{\rm BH}$ relates the distance and energy scales. Since P is dimensionless, it must be expressible as a function of dimensionless parameters, and, aside from λ_m, the ratio E_a/E_b is the only dimensionless parameter P can depend on. Note that P is also symmetric under $a \leftrightarrow b$.

Next we make the variable change $dE_a' dE_b' \to d\Delta d(E_a' + E_b')$ and use the energy delta function to integrate over $E_a' + E_b'$. Finally, with the same spirit that led to (39), we let

$$\int \frac{d\Delta}{|\Delta|^3} S \to \ln \Lambda \frac{d\delta(E_a - E)}{dE_a}\,, \tag{72}$$

and integrate once by parts, to obtain

$$R(E) = -16\pi^4 G^5 M_{\rm BH}{}^3 M_*{}^2 C^2 \ln \Lambda \frac{\partial}{\partial E}\left\{\int_0^\infty dE_b (EE_b)^{-1/2} P(E, E_b, \lambda_m)\right\}. \tag{73}$$

Because P depends only on E and E_b through their ratio, the curly-bracketed quantity is independent of E, as can easily be verified by changing the integration variable to E_b/E. Thus we have

$$R(E) \equiv 0 \tag{74}$$

for all E.

V. OBSERVABILITY

a) *Characteristic Parameters*

Four parameters, each having the dimensions of a length, characterize star counts or intensity measurements designed to detect a massive black hole. These parameters are a core radius r_c; a diaphragm size S; a "seeing" disk r_s of the optical telescope; and a characteristic gravitational capture radius r_h. Typical core radii, within which the unperturbed star distribution in a globular cluster is approximately constant, are (e.g., Peterson and King 1975):

$$r_c \sim 1 \text{ pc} \sim 20'' \,(\text{distance}/10 \text{ kpc})\,, \tag{75}$$

although all the four X-ray globular clusters that have been studied optically have $r_c \leq 0.5$ pc (Bahcall, Bahcall, and Weistrop 1975; Bahcall 1976). Typical diaphragm sizes within which one might wish to count stars and measure the light intensity (or velocity dispersions or profiles) are circles of radii of order

$$r_s \leqslant S \leqslant 10''\,, \tag{76}$$

where $r_s \sim 1''$ for ground-based observations and $\sim 0''.03$ for observations with a Large Space Telescope. The characteristic gravitational radius is (cf. eq. [3])

$$\begin{aligned} r_h &= 4.3 \times 10^{-2}\, \text{pc}(M_{\text{BH}}/10^3\, M_\odot)(10^2 \text{ km}^2 \text{ s}^{-2}/\langle \Delta v^2 \rangle) \\ &\sim 1 \text{ arcsec} \times (\text{distance}/10 \text{ kpc})^{-1} \left(\frac{M_{\text{BH}}}{10^3\, M_\odot}\right)\left(\frac{10^2 \text{ km}^2 \text{ s}^{-2}}{\langle \Delta v^2 \rangle}\right). \end{aligned} \tag{77}$$

For spectroscopic observations, another characteristic quantity enters:

$$v_0^2 = 2kT_{\text{star}}/M_{\text{star}}\,, \tag{78}$$

where T_{star} and M_{star} are appropriate averages of the stellar kinetic energies far from the black hole. The parameter v_0 is difficult to measure, but typical values may be of the order of 10 km s^{-1} for globular clusters (see, e.g., Peterson and King 1975; Illingworth and Freeman 1974). Nearer the black hole, the typical velocity v is of course much higher.

In what follows, we calculate various observable quantities as functions of dimensionless ratios of the above parameters.

b) *Number Density*

The number of stars per unit of volume is

$$n(r) = \int d^3v f(E, t)\,. \tag{79}$$

We assume, as a good approximation to our numerical solutions, that the distribution function is a factorable function of energy and eccentricity, i.e.,

$$f = \text{const. } E^{1/4} u(\lambda)\,. \tag{80}$$

By changing integration variables in equation (79) to $\lambda = (1 - \epsilon^2)/2$ and $y = rE/GM_{\text{BH}}$, one can show that

$$n(r) \propto r^{-7/4}\,, \tag{81}$$

independent of the distribution of eccentricities, $u(\lambda)$. A similar calculation gives $n \propto r^{-9/4}$ for the Peebles $p = \frac{3}{4}$ power law.

c) *Observability of a Density Cusp*

The numerical calculations of the distribution function that were performed using the time-dependent Boltzmann equation (see § III*d*) show that an approximate representation of the stellar density near the center of the star cluster is

$$n(r) \approx n_{\text{unperturbed}}(r)[1 + (r_h/r)^{7/4}]\,. \tag{82}$$

The number of stars that will appear in a circle of radius S is

$$N(S) = 4\pi \int_0^\infty dz \int_0^S x dx n(r)\,, \tag{83}$$

where we have chosen a cylindrical coordinate system with origin on the black hole. The polar axis z is oriented along the observer's line of sight, and x is the radial coordinate. Taking an approximate formula for the unperturbed star distribution (King 1962),

$$n_{\text{unperturbed}}(r) \approx \bar{n}(0)[1 + (r/r_c)^2]^{-3/2}\,, \tag{84}$$

we find (by numerical integration) that

$$N(S) \approx 2\pi\bar{n}(0)S^2 r_c[1 + 2.6(S/r_c)(r_h/S)^{7/4}]\,. \tag{85}$$

Equation (82) is valid for $S/r_c \leqslant 0.3$ and is the basic equation describing a density cusp.

If one had a telescope with infinitely good resolution, one could count individual stars in the innermost regions of a globular cluster and determine accurately the function $N(S)$. Unfortunately, with real telescopes (and a terrestrial atmosphere) the problem is much more difficult. We calculate now how massive a black hole would have to be to produce a definitely distinguishable stellar density cusp.

We suppose that one's "credibility threshold" for believing that a massive black hole is present is crossed if the number of stars within a radius S is F or more times the average star density in the cluster core (for most workers, $F \sim 3$ to 10). One finds, using equation (85), that the minimum gravitational radius r_h to which one is sensitive is then

$$r_h \approx 0.6(Fr_c)^{4/7}S^{3/7}\,. \tag{86}$$

Thus the maximum sensitivity is obtained by using the minimum diaphragm size consistent with a good signal-to-noise ratio. Diaphragms smaller than the seeing disk result in a loss of signal to noise. Thus the maximum sensitivity is achieved by choosing $S = r_s$.

Comparing equations (86) and (77) for plausible values of the parameters (Bahcall 1976; Peterson and King 1975), one finds that ground-based observations of globular clusters are sensitive to black-hole masses $\geqslant 5 \times 10^3\,M_\odot$ (for $F = 10$, $r_c \sim 5''$, $r_s \sim 1''$, $\langle\Delta v^2\rangle^{1/2} \sim 10\ \mathrm{km\ s^{-1}}$). For observations with a large space telescope, one might hope to detect black-hole masses as small as $10^3\,M_\odot$. The limit of detectability scales approximately as (cf. eqs. [3] and [86])

$$M_{\mathrm{BH}}(\text{detectable}) \propto r_{\text{core}}{}^{4/7}\langle\Delta v^2\rangle(\text{distance})^{+3/7}\,. \tag{87}$$

Note that one can search for the possible light enhancement just as well by using a photoelectric detector and integrating photons passing through a small diaphragm as by trying to count stars observed photographically close to the cluster center. In fact, the photoelectric measurement may be much easier and permits one to use smaller diaphragms. If one does observe a light enhancement photoelectrically, one can try to distinguish between the possibilities of many faint stars and one bright star (e.g., a horizontal-branch star) by taking spectra of the bright region or by trying to get high-resolution star counts close to the center.

We can illustrate the use of equation (85) by applying it to the case of M15 (= NGC 7078 = 3U 2131+11). From Figure 2 of Bahcall, Bahcall, and Weistrop (1975), we conclude that $2.6(S/r_c)(r_h/S)^{7/4}$ is $\leqslant 2$ at angular distances $S \geqslant 0'.05$. For a nominal core radius $r_c \sim 0'.1$–$0'.2$, one concludes that $r_h \leqslant 10''$ and (cf. eq. [77])

$$M_{\mathrm{BH}}(\text{in M15}) \leqslant 10^4\,M_\odot\,,$$

in agreement with the earlier results (Bahcall, Bahcall, and Weistrop 1975).

d) Velocity Dispersion and Line Profile

The velocity dispersion is higher for stars that are in bound orbits close to the black hole since the potential energy increases approximately as r^{-1} near the center of the cluster. The velocity dispersion that one would expect to measure in a diaphragm of radius S centered on the black hole (cf. eq. [83]) is

$$\langle v_z{}^2\rangle_{\text{diaphragm}} = \frac{\int_0^\infty dz \int_0^S xdxn(r)\int v_z{}^2[f_{E<0} + f_{E>0}]d^3v}{\int_0^\infty dz \int_0^S xdxn(r)\int (f_{E<0} + f_{E>0})d^3v}\,, \tag{88}$$

where x and z have the meaning described before (eq. [83]) and $n(r)$ is the undisturbed star distribution represented approximately by equation (84). Using the distribution function $f_{E>0} \propto E^{1/4}$, the Gaussian distribution function $f_{E<0}$ of equation (50), and the relative normalization indicated by equation (61), one can show that

$$\langle v_z{}^2\rangle_{\text{diaphragm}} = \langle\Delta v^2\rangle \frac{\int_0^\infty dz \int_0^S xdxn[(1 - P(5/2, a))e^{+a} + 0.4(a)^{11/4}]}{\int_0^\infty dz \int_0^S xdxn[(1 - P(3/2, a))e^{+a} + 1.1(a)^{7/4}]}\,. \tag{89a}$$

In the above equation, $a \equiv r_h/r$ and $P(n, a)$ is the normalized incomplete gamma function of index n,

$$P(n, a) = \Gamma(n)^{-1}\int_0^a \exp(-t)t^{n-1}dt\,. \tag{89b}$$

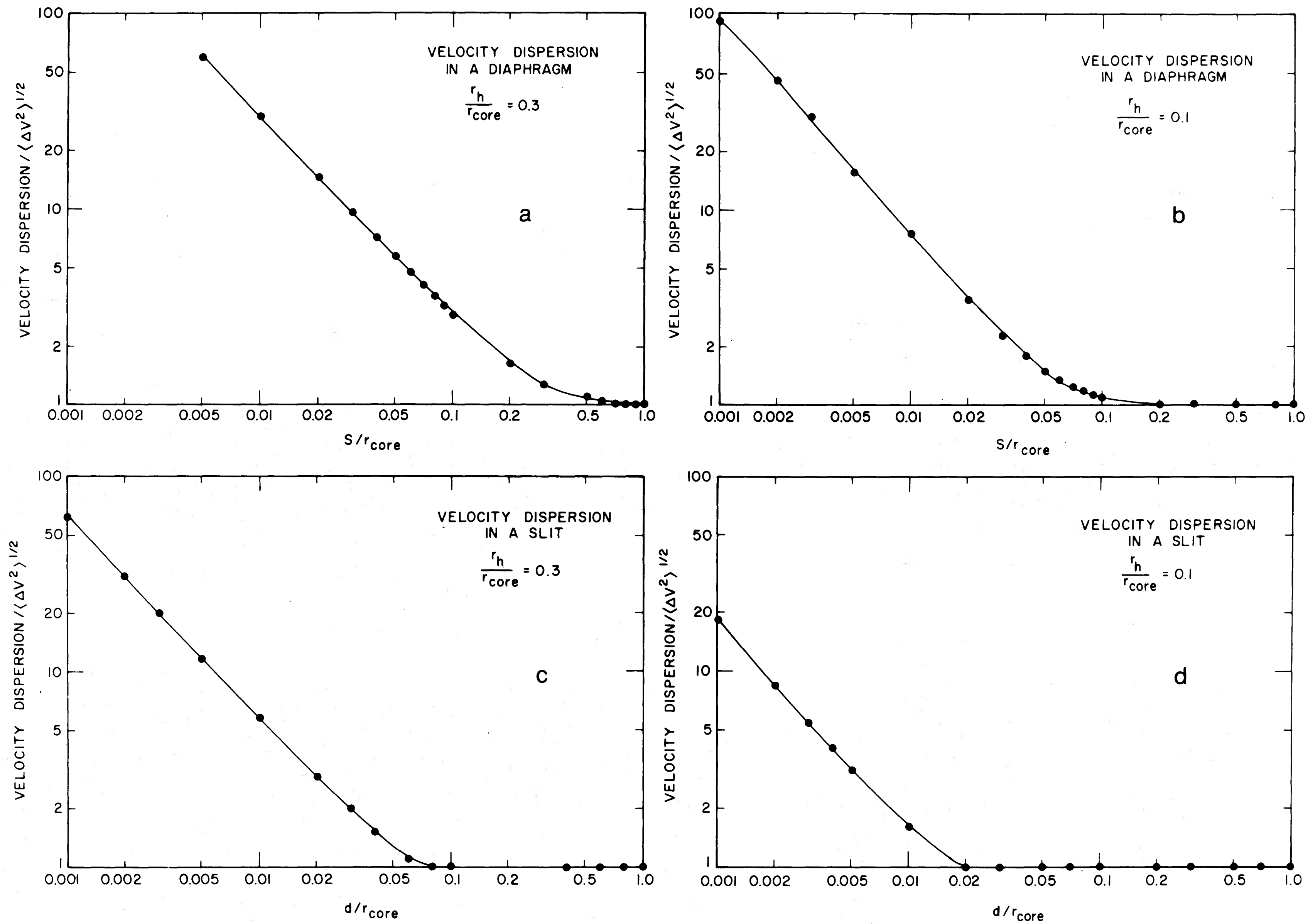

FIG. 3.—(*a*) and (*b*) Velocity dispersion expected with measurements using a diaphragm of radius S (cf. eq. [89]). (*c*) and (*d*) The velocity dispersion that would be measured along an "ideal" slit for two typical cases (cf. eq. [91]).

We have evaluated equation (89) numerically; the results for the calculated velocity dispersions are shown in Figures 3*a* and 3*b* for some typical cases. One can also derive an approximate analytic expression that provides a reasonably good representation (typically $\sim 10\%$ accuracy in the regions of interest) of the numerical calculations. We find

$$\langle v_z^2 \rangle_{\text{diaphragm}} \approx \frac{[0.9 + 3.5(r_h/r_{\text{core}})(r_h/S)^{7/4}]}{[0.8 + 3.0(r_h/r_{\text{core}})(r_h/S)^{3/4}]} \langle \Delta v^2 \rangle . \tag{90}$$

We see from Figure 3 and equation (90) that there are appreciable effects ($\gtrsim 50\%$) of the black hole on the velocity dispersion for $r_h \gtrsim 2S$.

Formulae (88)–(90) apply to the velocity dispersion of individual stars within a circular diaphragm of radius S. In practice, it may be easier to study the velocity dispersion as obtained from a series of open slit spectra placed close to or on the center of the globular cluster. The width of the slit, in the direction of the dispersion, would typically be of the order of the seeing disk, r_S, while the length of the slit might be as large as r_{core}. We calculate below the velocity dispersion that would be observed with an "ideal" slit (width $\ll$ length; no effects of seeing included) and indicate how these results might be used in practice.

The velocity dispersion that would be measured with an ideal slit is

$$\langle v_z^2 \rangle_{\text{ideal slit}, d} = \frac{\int_0^\infty dz n(r) \int [f_{E<0} + f_{E>0}] v_z^2 d^3\boldsymbol{v}}{\int_0^\infty dz n(r) \int [f_{E<0} + f_{E>0}] d^3\boldsymbol{v}} , \tag{91}$$

where

$$r^2 = z^2 + d^2 + y^2 \tag{92}$$

and d is the distance along the length of the slit from the center of the cluster and $y(\ll d)$ is some "average" width of the slit. The integrations over velocity can be carried out analytically (cf. eq. [89a]), and the remaining one-dimensional integrations are simple to perform numerically. The results are shown in Figures 3*c* and 3*d* for some typical cases. An approximate analytic representation is

$$\langle v_z^2 \rangle_{\text{slit}} \approx \frac{1 + 0.45(r_h/r_c)(r_h/d)^{7/4}}{1 + 2.1(r_h/r_c)(r_h/d)^{3/4}} \langle \Delta v^2 \rangle . \tag{93}$$

Note that Figures 3*c* and 3*d*, and equation (94), suggest that there is a 50 percent effect of the black hole on the velocity dispersion only when $r_h \sim 10d$.

There is no discrepancy between this result and the analogous relation given in equation (91) for a diaphragm. The integration over x (or equivalently, d) used to obtain the results for a diaphragm allow contributions from distances much closer to the black hole than the minimum diaphragm size, $S(= r_S)$. Since the velocity dispersion increases approximately as r^{-1} (see below), these closer contributions are weighted more heavily in the diaphragm average than are the outer contributions. In practice, a real slit spectrum will also contain contributions at a distance d from stars at closer separations because of seeing effects. For a slit spectrum at $d \sim r_S$, where the most critical information is obtained, the expected result is reasonably well approximated by the calculations described earlier for a diaphragm. For $d \gg r_S$, one can use the results of Figures 3*c* and 3*d*, or equation (94), but must average them over seeing effects and the width of the slit.

The one-dimensional velocity dispersion at a specified radius is given by the ratio of bracketed quantities in equation (89a). For some purposes, it is convenient to have an approximate analytic formula for the velocity dispersion of the bound stars; one finds

$$\langle v_z^2 \rangle_{\text{at } r} \approx \tfrac{4}{11} \langle \Delta v^2 \rangle (r_h/r) , \tag{94}$$

for $r_h \gg r \gg r_D$. Near $r = r_D$, the actual velocity dispersion may be of order a factor of 2 larger than indicated by equation (94).

For possible applications, it is important to know if the velocity dispersions calculated above for a slit and a diaphragm are associated with a fairly "normal" line profile. The line profile can be determined from the following expression:

$$I(v_z^2, M_{\text{BH}}, S) = I_0 \int dz \int x dx \int [f_{E<0} + f_{E>0}] v_\perp dv_\perp , \tag{95}$$

where $v_\perp$ is the magnitude of the velocity perpendicular to the line of sight. The calculation of the line profile using equation (95) is complicated since one must use various ranges of integration depending on the relative sizes of r, r_h, GM_{BH}/v_z^2, S, and r_c. The final result must be obtained by one-dimensional numerical integrations. The results are shown in Figures 4*a*–4*d* for some typical cases. An expression for the line profile involving just one-dimensional integrals is given in Appendix A.

It can be seen from Figures 4*a*–4*d* that the expected velocity profile has broad wings; much of the calculated contribution to the velocity dispersion (eqs. [89]–[93]) comes from these wings. Since the measurement of wings

1976ApJ...209..214B

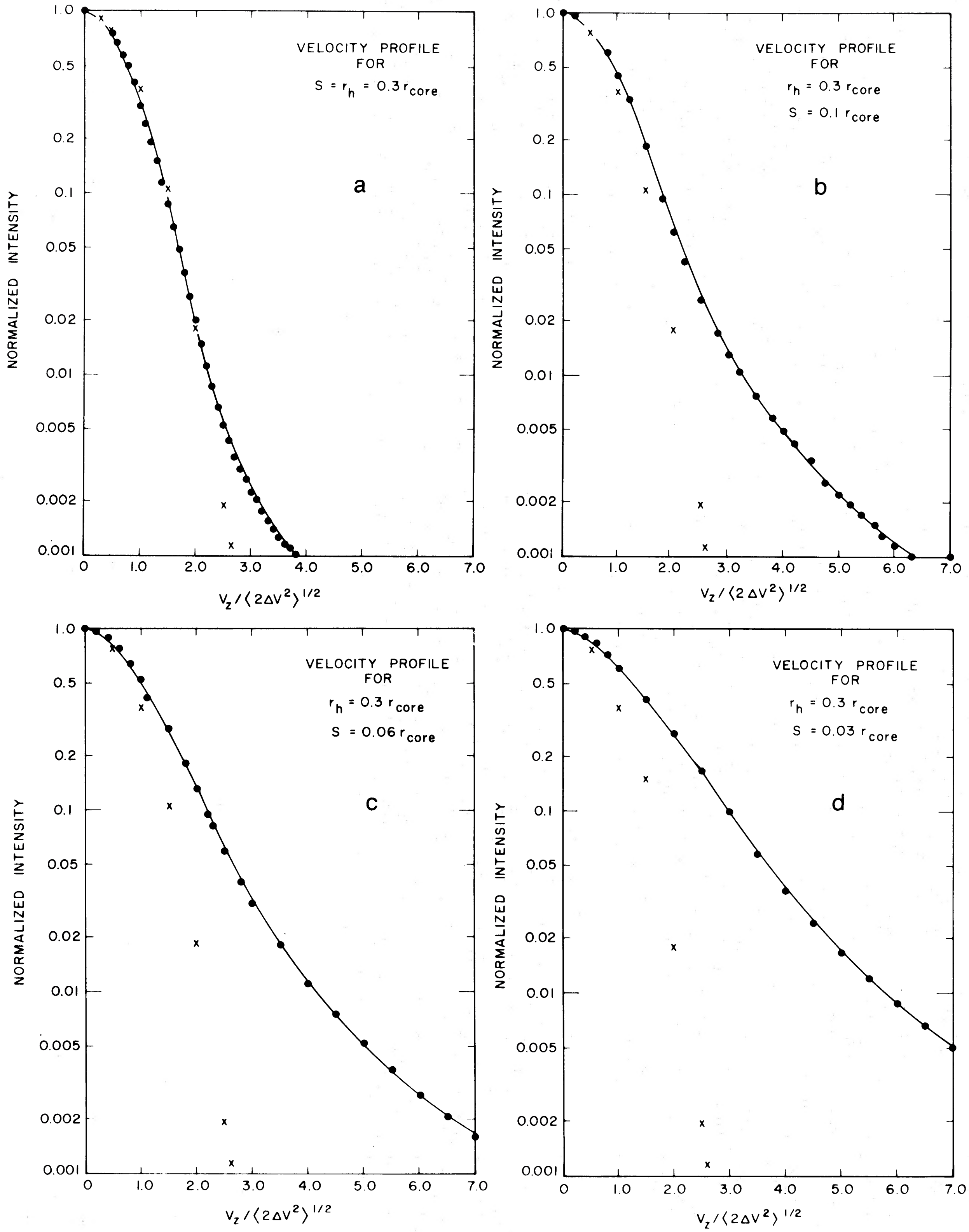

FIG. 4.—The expected velocity profile as calculated for a diaphragm of radius S (cf. eq. [95] and Appendix A). The dots represent the velocity profile in the presence of a black hole and the crosses represent the profile with no black hole present.

in the velocity profile of an absorption line, or the detection of occasional high-velocity stars, is rather difficult observationally, we estimate a minimum detectable black-hole mass as given by (cf. Figs. 4 and Appendix A)

$$r_{h,\,\mathrm{min}} \sim 5 r_S \,, \tag{96}$$

where r_S is the seeing disk. For $r_h \sim 5r_S$, there are appreciable differences between the expected velocity profile with and without a massive black hole present even at velocities $\sim\langle 2\Delta v^2\rangle^{1/2}$. Note that the minimum mass detectable spectroscopically depends linearly on the size of the seeing disk; number counts or intensity measurements depend instead on $r_S^{3/7}$ (see eq. [86]).

One might hope to detect black-hole masses $\gtrsim 5 \times 10^3\, M_\odot$ with ground-based spectroscopic observations and masses as small as $5 \times 10^2\, M_\odot$ with a Large Space Telescope. The above estimates are based on plausible but uncertain choices of the parameters (cf. eq. [77], $\langle \Delta v^2\rangle^{1/2} \sim 10$ km s^{-1}, $r_S \sim 1''$ or $0''.1$, respectively, for ground or space observations).

e) *Location of the Black Hole*

A massive black hole should be close to the center of the star distribution in a globular cluster since this is the region of lowest gravitational potential. It is useful to estimate the mean distance, $\langle r\rangle$, of a massive star (black hole or otherwise) from the center of the cluster; future X-ray observations might be able to distinguish between various models of the globular-cluster X-ray sources depending on the observed values of $\langle r\rangle$ (Clark 1975). A correct treatment of this problem would involve the solution of the appropriate Fokker-Planck equation for the probability distribution of r in the presence of both bound and unbound stars. Instead we present a simple estimate that ignores all unbound stars as well as the polarizing effects of the black hole on the surrounding stellar medium. This simplified treatment was developed in collaboration with A. Lightman.

With the above-described approximations, the average separation of the massive object, M_{X}, from the stellar center is

$$\langle r\rangle \approx \int_0^\infty drr^3 \exp\left(-M_{\mathrm{X}}\phi(r)/M_*\langle\Delta v^2\rangle\right) \Big/ \int_0^\infty drr^2 \exp\left(-M_{\mathrm{X}}\phi(r)/M_*\langle\Delta v^2\rangle\right) \tag{97}$$

or

$$\langle r\rangle \approx \left[\frac{8M_*\langle\Delta v^2\rangle}{\pi M_{\mathrm{X}}\phi''(0)}\right]^{1/2}, \tag{98}$$

where $\phi''(0)$ is the Laplacian of the gravitational potential at the center of the cluster.

For the unperturbed star-distribution given in equation (84),

$$\phi(r) \approx -(6GM_{\mathrm{core}}/r_c)[1 - 6^{-1}(r/r_c)^2] \tag{99}$$

and

$$\langle\Delta v^2\rangle \approx 0.65 GM_{\mathrm{core}}/r_c \,, \tag{100}$$

so

$$\langle r\rangle \approx 0.9 r_c (M_*/M_{\mathrm{X}})^{1/2} \,. \tag{101}$$

The standard deviation $\langle (r - \langle r\rangle)^2\rangle^{1/2}$, is

$$\sigma(\langle r\rangle) = \langle r\rangle((3\pi - 8)/8)^{1/2} \approx 0.42\langle r\rangle \,. \tag{102}$$

For all the globular-cluster X-ray sources that have been studied optically so far, $r_c \lesssim 5''$ (Bahcall 1976). Many models of these X-ray sources, including some involving binary systems, suggest that $M_{\mathrm{X}} \gtrsim 10\, M_\odot$ and thus $\langle r\rangle \lesssim 1''$. Therefore, these models predict that the X-ray source should be located at the center of the unperturbed star distribution within the foreseeable accuracy of the measurements.

It is useful to rewrite equation (101) in terms of r_h using equations (3) and (100). One finds:

$$\langle r\rangle \approx 0.6 r_h (M_c/M_{\mathrm{X}})[M_*/M_{\mathrm{X}}]^{1/2} \,. \tag{103}$$

For $M_{\mathrm{X}} < 10^{2.5}\, M_\odot$, the X-ray source spends most of its time in regions where the stars are in thermal equilibrium with a kinetic temperature $kT_* \sim M_*\langle\Delta v^2\rangle$ and equations (97)–(103) are therefore reasonable approximations. For larger values of M_{X}, the above analysis is not applicable, but the correct values of $\langle r\rangle$ are too small to be measurable with known techniques.

VI. LARGE STATISTICAL FLUCTUATIONS

The total number of stars with $r < r_1 \ll r_h$ is, according to equations (77) and (82),

$$N(r < r_1) \approx (40 \text{ stars})(r_1/r_h)^{5/4}[n_0/5 \times 10^4 \text{ pc}^{-3}][M_{\mathrm{BH}}/10^3\, M_\odot]^3[100 \text{ km}^2\text{ s}^{-2}/\langle\Delta v^2\rangle]^3 \,. \tag{104}$$

The radius containing one star, on the average, is given by

$$r_* \approx (0.05 r_h)[n_0/5 \times 10^4 \text{ pc}^{-3}]^{-0.8}\left[(10^3\, M_\odot/M_{\rm BH})\frac{\langle \Delta v^2\rangle}{100 \text{ km}^2 \text{ s}^{-2}}\right]^{2.4} . \tag{105}$$

Applications involving the use of our computed distribution functions in the region $r \lesssim r_*$ are numerically unreliable since statistical fluctuations about the ensemble-average are likely to be large.

VII. ACCRETION RATE

Bahcall and Ostriker (1975) suggested that, among other likely processes, globular-cluster X-ray sources may be powered by accretion of matter from stars that are tidally disrupted by passage close to the black hole, a rate we calculate in § III*e*, equation (65). For larger black-hole masses ($M_{\rm BH} > 10^3\, M_\odot$), the process of gravitational diffusion may be more important, especially when loss-cone effects are included. The accretion rate for gravitational diffusion is proportional to $M_{\rm BH}^3$ compared to $M_{\rm BH}^{4/3}$ for tidal disruption (cf. equations (62c) and (64) with equation (65)).

The time for the mass of the black hole to double (from $M_{\rm BH}$ to $2\, M_{\rm BH}$) by the accretion of tidally disrupted stars is

$$t_{\text{double, tidal}} \approx 2 \times 10^{10} \text{ yr}\left[\left(\frac{10^3\, M_\odot}{M_{\rm BH}}\right)^{1/3}\left(\frac{5 \times 10^4 \text{ pc}^{-3}}{n_0}\right)\left(\frac{\langle \Delta v^2\rangle^{1/2}}{10 \text{ km s}^{-1}}\right)\right] , \tag{106}$$

where we have indicated only the most important dependencies. A lower-limit time for doubling by gravitational diffusion can be crudely estimated from equation (62c):

$$t_{\text{double, diffusion}} \sim 2 \times 10^9 \text{ yr}\left[\left(\frac{10^3\, M_\odot}{M_{\rm BH}}\right)^2\left(\frac{5 \times 10^4 \text{ pc}^{-3}}{n_0}\right)^2\left(\frac{\langle \Delta v^2\rangle^{1/2}}{10 \text{ km s}^{-1}}\right)^9\right] . \tag{107}$$

The estimate given in equation (107) may be one or two orders of magnitude too small if the actual diffusion rate is nearer that given by the numerical solutions of the time-dependent diffusion equation, cf. equation (64). The latter equation could be used to find an upper limit to the doubling time by diffusion.

We are grateful to Karl Rubin for expert programming and mathematical assistance and to Y. Avni, F. Dyson, B. Flannery, J. Katz, A. Lightman, J. Ostriker, P. J. E. Peebles, W. Press, M. Rees, and M. N. Rosenbluth for valuable conversations and for suggestions that greatly improved various drafts of this paper.

APPENDIX A

The velocity profile defined by equation (95) can be written in a fairly simple form after carrying out some algebra. Let $v_0 \equiv \langle 2\Delta v^2\rangle^{1/2}$, $r_z = 2GM_{\rm BH}/v_z^2$, $r_0 = 2GM_{\rm BH}/v_0^2$, and $\theta(x) = 1$ for $x > 0$ and $\theta(x) = 0$ for $x < 0$. We assume, as a reasonable approximation, that $n(r) = \text{constant} \times \theta(r_c - r)$. As before, r_c and S are, respectively, the unperturbed core radius and diaphragm size. One finds

$$I = \text{constant}(I_1 + I_2 + I_3 + I_4 + I_5) ,$$

where

$$I_1 = [\theta(S - r_z) r_z^3/3] ,$$

$$I_2 = [\theta(r_z - S)/3]\{\theta(r_z - r_c)[r_c^3 - (r_c^2 - S^2)^{3/2}] + \theta(r_c - r_z)[r_z^3 - (r_z^2 - S^2)^{3/2}]\} ,$$

$$I_3 = [\theta(r_c - r_z) 8 r_0^3/5]\int_0^{(v_0/v_z)^2} dy y^{3/4}(1 - v_z^2 y/v_0^2)^{5/4}\left\{1 - \theta\left(y - \frac{S}{r_0}\right)\left[1 - \left(\frac{S}{y r_0}\right)^2\right]^{1/2}\right\} ,$$

$$I_4 = \{\theta(r_c - r_z) r_0^3 \exp[-(v_z/v_0)^2]\}\int_{(v_0/v_z)^2}^{(r_c/r_0)} dy y^2 \exp(y^{-1})\left\{1 - \theta\left(y - \frac{S}{r_0}\right)\left[1 - \left(\frac{S}{y r_0}\right)^2\right]^{1/2}\right\} ,$$

and

$$I_5 = [8\theta(r_z - r_c)\theta(r_z - S) r_0^3/5]\int_0^{(r_c/r_0)} dy y^{3/4}[1 - (v_z/v_0)^2 y]^{5/4}\left\{1 - \theta\left(y - \frac{S}{r_0}\right)\left[1 - \left(\frac{S}{y r_0}\right)^2\right]^{1/2}\right\} .$$

REFERENCES

Bahcall, J. N., Bahcall, N. A., and Weistrop, D. 1975, *Ap. Letters*, **16**, 159.
Bahcall, J. N., and Ostriker, J. P. 1975, *Nature*, **256**, 23.
Bahcall, N. A. 1976, *Ap. J.* (*Letters*), **204**, L83.
Canizares, C. R., and Neighbours, J. E. 1975, *Ap. J.* (*Letters*), **199**, L97.

Chandrasekhar, S. 1942, *Principles of Stellar Dynamics* (Chicago: University of Chicago Press; reprinted by Dover Publications, New York).
———. 1943, *Rev. Mod. Phys.*, **15**, 1.
Clark, G. W. 1975, private communication.
Clark, G. W., Markert, T. H., and Li, F. K. 1975, *Ap. J.* (*Letters*), **199**, L93.
Cohen, R. S., Spitzer, L., and Routly, P. McR. 1950, *Phys. Rev.*, **80**, 230.
Frank, J. 1976, to be published.
Giacconi, R., Murray, S., Gursky, H., Kellogg, E., Schreier, E., Matilsky, T., Koch, D., and Tananbaum, H. 1974, *Ap. J. Suppl.*, No. 237, **24**, 37.
Hills, J. G. 1975, *Nature*, **254**, 295.
Illingworth, G., and Freeman, K. C. 1974, *Ap. J.* (*Letters*), **188**, L83.
King, I. R. 1962, *A.J.*, **67**, 471.
Peebles, P. J. E. 1972*a*, *Gen. Rel. and Grav.*, **3**, 63.
———. 1972*b*, *Ap. J.*, **178**, 371.
Peterson, C. J., and King, I. R. 1975, *A.J.*, **80**, 427.
Rosenbluth, M. N., MacDonald, W. M., and Judd, D. L. 1957, *Phys. Rev.*, **107**, 1.
Silk, J., and Arons, J. 1975, *Ap. J.* (*Letters*), **200**, L131.
Spitzer, L., and Hart, M. H. 1971, *Ap. J.*, **169**, 399.
Wyller, A. A. 1970, *Ap. J.*, **160**, 443.

John N. Bahcall: Institute for Advanced Study, Princeton, NJ 08540

R. A. Wolf: Department of Space Physics and Astronomy, Rice University, Houston, TX 77001